JPET Fast Forward. Published on June 12, 2012 as DOI: 10.1124/jpet.112.192203

Vidofludimus Inhibits Colonic IL-17 and Improves Hapten-Induced Colitis in Rats by a Unique Dual Mode of Action

Leo R. Fitzpatrick, Jeffrey S. Small, Robert Doblhofer, Aldo Ammendola

Primary Laboratory of Origin: Fitzpatrick Laboratory, Department of Pharmacology, Penn State College of Medicine.

Author Affiliations: Department of Pharmacology, Penn State College of Medicine, Hummelstown, PA 17036 (USA) [LRF, JSS]. 4SC AG, 82152 Planegg-Martinsried, (Germany) [RD, AA].

JPET Fast Forward. Published on June 12, 2012 as DOI: 10.1124/jpet.112.192203
This article has not been copyedited and formatted. The final version may differ from this version.

Running Title: Vidofludimus Improves Colitis in Rats by Dual Mechanism

Corresponding Author: Leo R. Fitzpatrick Ph.D., Department of Pharmacology, Penn State College of Medicine, Hummelstown, PA 17036 (USA). Telephone: (717) 531-0393, Fax: (717) 531-1046, Email: lfitzpatrick@psu.edu

Manuscript Length: 32 pages

Number of Tables = 0

Number of Figures = 9

Number of References = 35

Number of Words in Abstract = 249

Number of Words in Introduction = 524

Number of Words in Discussion = 1677

Nonstandard Abbreviations: Vido (Vidofludimus), Uridine (Uri), dihydroorotate dehydrogenase (DHODH), Proliferating cell nuclear antigen (PCNA), Terminal deoxynucleotidyl transferase dUTP nick end labeling (TUNEL)

Recommended Section Assignment: Inflammation, Immunopharmacology and Asthma

JPET Fast Forward. Published on June 12, 2012 as DOI: 10.1124/jpet.112.192203
This article has not been copyedited and formatted. The final version may differ from this version.

Abstract

Vidofludimus (Vido) is a novel oral immunomodulatory drug that inhibits dihydroorotate dehydrogenase and lymphocyte proliferation *in vitro*. Vido inhibits IL-17 secretion *in vitro* independently of effects on lymphocyte proliferation. **Aim:** Our primary goal was to evaluate the *in vivo* effects of Vido on IL-17 secretion and parameters of TNBS-induced colitis in rats. Secondarily, to further delineate the mechanism of action for Vido, rats were dosed concomitantly with Uridine (Uri). **Methods:** Young Wistar rats received a 150 µL enema of either PBS or TNBS on study day 1. The *ex vivo* effects of Vido on 24-hour colonic IL-17 secretion were determined using colonic strips from PBS or TNBS treated rats. Some rats were dosed with vehicle, Vido or Vido + Uri for a six-day period. On day 6, parameters of colitis were determined from colonic tissue. These parameters included macroscopic, histological, and transcription factor measurements, IL-17 production and numbers of CD3+ T cells. **Results:** *Ex vivo*, Vido completely blocked IL-23 + IL-1β stimulated secretion of IL-17 by colonic strips. *In vivo*, Vido treatment alone most effectively reduced macroscopic and histological pathology, and numbers of CD3+ T cells. In contrast, similarly reduced nuclear STAT3 binding and IL-17 levels were observed from animals treated with Vido alone and Vido + Uri. **Conclusions:** Vido improves TNBS-induced colonic inflammation by a unique dual mode of action: 1) inhibiting expansion of colonic T-lymphocytes, and 2) suppressing colonic IL-17 production, which is independent from the control of T-lymphocyte proliferation, by inhibition of STAT3 and NF-κB activation.

JPET Fast Forward. Published on June 12, 2012 as DOI: 10.1124/jpet.112.192203
This article has not been copyedited and formatted. The final version may differ from this version.

Introduction

More optimal pharmacological approaches are still needed for the treatment of inflammatory bowel disease (IBD), and in particular for patients with Crohn's disease [CD] (Holtmann and Neurath, 2006; Lanzarotto et al., 2006). Some patients with moderate to severe CD are intolerant to and/or non responsive to azathioprine/6-mercaptopurine, as well as anti-TNF-α antibodies (Prajapati et al., 2003; Holtmann et al. 2008). Therefore, other immunomodulatory drugs (including Vidofludimus) have been investigated in clinical trials for the treatment of IBD (Prajapati et al., 2003; Holtmann et al. 2008, Herrlinger et al. 2011).

Vidofludimus (4SC-101) is a potent inhibitor of dihydroorotate dehydrogenase (DHODH), which is a key enzyme involved in pyrimidine biosynthesis. (Fitzpatrick et al, 2010a; Kulkarni et al., 2010). Most mammalian cells recruit uridine by recycling through a salvage pathway. In contrast, activated lymphocytes synthesize 4 to 8 fold more pyrimidines, and utilize the *de novo* biosynthetic pathway (Ruckemann et al., 1998; Fox et al., 1999). Because of its capability to inhibit DHODH, Vidofludimus (designated here as Vido) can inhibit leukocyte proliferation (Fitzpatrick et al., 2010a; Kulkarni et al., 2010). However, previously we showed that Vido inhibits IL-17 secretion by peripheral blood mononuclear cells (PBMC's) independently of effects on cellular proliferation (Fitzpatrick et al., 2010a). Specifically, we found that the inhibitory effects of Vido on cellular proliferation could be reversed in the presence of exogenous uridine (designated here as Uri) (Fitzpatrick et al., 2010a). In contrast, Uri could not reverse the inhibitory effect of Vido on PHA stimulated IL-17 secretion by PBMC's. Moreover, we also reported that Vido attenuates IL-17 secretion from cytokine-stimulated murine splenocytes, by inhibiting STAT3 and NF-KB signaling pathways in these cells (Fitzpatrick et al., 2011a). As a whole, these data suggest that Vido may have a dual mode of immunomodulatory action *in vitro*: 1) inhibition of leukocyte proliferation, and 2) inhibition of IL-17 secretion, which is unrelated to leukocyte proliferation (Fitzpatrick et al., 2010a; 2010; Fitzpatrick et al., 2011a).

JPET Fast Forward. Published on June 12, 2012 as DOI: 10.1124/jpet.112.192203
This article has not been copyedited and formatted. The final version may differ from this version.

Of relevance to this manuscript, we also reported that Vido could effectively improve both chronic dextran sulfate sodium (DSS)-induced colitis, as well as acute hapten (trinitrobenzene sulfonic acid [TNBS])-induced colitis, in mice (Fitzpatrick et al., 2010a). Moreover, Vido attenuated the activation of STAT3 and NF-κB signaling pathways in the colons of TNBS-treated mice, and also inhibited the production of IL-17 (Fitzpatrick et al., 2010a, Fitzpatrick et al., 2011a). These anti-colitis actions of Vido may reflect the inhibition of leukocyte proliferation and/or the direct inhibition of IL-17, by modulating relevant intracellular signal-transduction systems (Fitzpatrick et al., 2010a; Fitzpatrick et al., 2011a).

With a knowledge of this background information, our primary goal was to evaluate the effects of Vido on colonic IL-17 secretion (*ex vivo* and *in vivo*), as well as the pharmacological effects on various parameters of TNBS-induced colitis in rats. Included in these parameters was the measurement of CD3+ T cell numbers in the rat colon. Secondarily, to help further delineate the mechanism(s) of anti-colitis action for Vido, rats were dosed in the presence or absence of exogenous Uri. Other investigators have used this approach to examine the *in vivo* mode of action for leflunomide (another DHODH inhibitor) in rats (Chong et al., 1999).

JPET Fast Forward. Published on June 12, 2012 as DOI: 10.1124/jpet.112.192203
This article has not been copyedited and formatted. The final version may differ from this version.

Methods

Key Chemicals

Vidofludimus was provided by 4SC AG (Planegg-Martinsried, Germany). The chemical structure of this compound can be found in a prior publication (Fitzpatrick et al., 2010a). Recombinant rat IL-1β and IL-23 were obtained from R&D Systems (Minneapolis, MN). Key reagents for the myeloperoxidase (MPO) assay such as (3, 3′, 5, 5′ tetramethylbenzidine [TMB], hexadecyltrimethylammoniun bromide [HTAB]) and N, N dimethylformamide were obtained from Sigma Chemical Company (Saint Louis, MO). TNBS and uridine were also obtained from Sigma. The rat IL-17 ELISA kit was obtained from eBioscience Inc. (San Diego, CA). The CD3 and PCNA antibodies were obtained from abcam (Cambridge, MA). The Vectastatin Elite Kit, which was used for immunohistochemistry studies, came from Vector Laboratories (Burlingame, CA). The ApopTag® peroxidase in situ apoptosis detection kit and Proteinase K was obtained from Millipore (Billerica, MA).

Animals

Timed pregnant female Wistar rats were purchased from Charles River Laboratories Inc. (Wilmington, MA). Animals were housed under standard conditions with a 12-hour light-dark cycle. Both male and female weanling rats were used in these studies. The average weight of these rats on postnatal day 23 was 62.1 ± 0.9 grams.

Colonic Organ Culture for Determining IL-17 Secretion

Young rats (four weeks old, n = 3 per group) that had been treated with one intracolonic treatment of PBS or TNBS (see below) were utilized for colonic organ culture experiments, as described by other investigators (Tanabe et al., 2008). Briefly, five days after the intracolonic instillation of PBS or TNBS, multiple distal colonic strips (n = 11 to 12 per treatment group) of

JPET Fast Forward. Published on June 12, 2012 as DOI: 10.1124/jpet.112.192203
This article has not been copyedited and formatted. The final version may differ from this version.

standard size (3 mm) were cultured for 24 hours in culture medium that contained an antibiotic-antimycotic cocktail (Life Technologies, Grand Island NY). This antibiotic-antimycotic solution contained 100 units/ml of penicillin, 100 µg/ml of streptomycin and 0.25 µg/ml of amphotericin B. The These colonic strips were treated with: no cytokines, cytokine treatment [rat IL-23 (10 ng/ml) + rat IL-1β (10 ng/ml)], or cytokine treatment + Vidofludimus (25, 50 or 100 µM). IL-17 secretion was measured from the culture medium by ELISA.

TNBS-Induced Colitis in Rats

Essentially, we utilized the acute version of the TNBS-induced colitis model, which was described previously by our laboratory (Fitzpatrick et al., 2010b). Briefly, on postnatal day 22, newly weaned rats (both sexes) were dosed with vehicle(s) (Phosal 50 PG [p.o.] or 0.9% saline [i.p.]), Uridine (500 mg/kg, i.p.), Vidofludimus (60 mg/kg, p.o.), or Vidofludimus (60 mg/kg, p.o.) + Uridine (500 mg/kg, i.p.). There were 4 to 8 rats in each treatment group. The dose volumes for Phosal 50 PG and other p.o. treatments were 5 ml/kg. The dose volumes for saline and uridine treatments were also 5 ml/kg. These animals were dosed for a six day period (postnatal days 22-27). On postnatal day 23, rats received a 150 µL enema of either PBS or TNBS (8 mg in 40% Ethanol/PBS). On day 28, rats were euthanized by exposure to carbon dioxide. The colons were collected for the measurement of various colitis indices (see below), as described previously (Fitzpatrick et al., 2010a: Fitzpatrick et al., 2010b).

Macroscopic Colonic Score

The macroscopic scores were determined by the method of Reuter et al., as described previously by our laboratory (Reuter et al., 1996; Fitzpatrick et al., 2010a). The scoring system involves a combination of various features: ulceration, adhesions, colonic thickness, loose stool/diarrhea. The macroscopic ulcer component was scored according to the following criteria: 0 = normal appearance, 1 = focal hyperemia, no ulcers, 2 = ulceration without hyperemia or

JPET Fast Forward. Published on June 12, 2012 as DOI: 10.1124/jpet.112.192203
This article has not been copyedited and formatted. The final version may differ from this version.

bowel wall thickening, 3 = ulceration with inflammation at one site, 4 = ulceration/inflammation at two or more sites, 5 = major sites of damage extending > 1 cm along the length of colon, 6-10 = when damage extends > 2 cm along the colon, the score is increased by 1 for each additional cm of involvement (Reuter et al., 1996; Fitzpatrick et al., 2010a).

Colonic Histology Score

For the colonic histology evaluations, we utilized two segments (both approximately 1.5 cm in length) of the distal colon from each animal. Therefore, these samples encompassed relevant areas of macroscopic colonic damage, if present (Fitzpatrick et al., 2010a). Histological evaluations were performed on coded H&E stained slides. Two slides from the distal colon were examined per animal. The colonic histology scores were determined by the method of Elson et al. on a 12-point severity scale, as described previously (Elson et al., 1996; Fitzpatrick et al., 2010a).

Colonic MPO and IL-17 Assays

These parameters were measured by standard methods described previously by our laboratory (Fitzpatrick et al., 2010a; Fitzpatrick et al., 2010b). These results were expressed as the fold change compared to the PBS treatment group.

Immunohistochemistry

Generally, we followed the procedures for immunohistochemistry with colonic tissue samples, which have been described previously by our laboratory (Fitzpatrick et al., 2010a; Fitzpatrick et al., 2010b). For determining the number of CD3 positive T cells, we utilized coded slides and counted (at a magnification 600x) the number of positively DAB-stained cells within six areas of the colonic lamina propria and submucosa. The average number of positively stained cells was

JPET Fast Forward. Published on June 12, 2012 as DOI: 10.1124/jpet.112.192203
This article has not been copyedited and formatted. The final version may differ from this version.

then determined for each slide (i.e., colonic specimen). Subsequently, the results were expressed as the mean numbers of CD3+ cells per individual treatment groups.

For examining leukocyte proliferation, we used the proliferating cell nuclear antigen (PCNA) immunohistochemistry method. We evaluated two slides per treatment group. This method has been used previously in conjunction with the rat TNBS colitis model (Nakase et al., 2001).

Assessment of Apoptosis (TUNEL Method)

The TUNEL method was used to determine leukocyte apoptosis in the colonic lamina propria and submucosa. Generally, we utilized the method described previously in our laboratory (Fitzpatrick et al., 2011b). This method has been used previously in conjunction with the TNBS colitis model (Wittig et al., 2000). Briefly, slides (two per treatment group) were immersed in xylene to remove paraffin. After washes in successively lower concentrations of ethanol, the sections were permeabilized with 0.3% Triton X-100/PBS, followed by Proteinase K. Subsequently, the sections were quenched in 3% hydrogen peroxide, followed by successive applications of various components (Equilibration buffer, TdT and anti-digoxigenin conjugate) provided with the apoptosis detection kit. After application of DAB substrate (10 minutes), and brief counterstaining with Gill's hematoxylin (30 seconds), aqueous mounting solution was applied to the slides.

Western Blot Analysis

Nuclear extracts from the distal colon were used for assessing NF-κB p65 expression. A protein determination was done with the Bio-Rad protein assay. Overall, we followed the western blot procedure described previously by our laboratory (Fitzpatrick et al., 2008). For these western blot analyses, we used 40 μg of protein. We utilized a rabbit polyclonal antibody (ab 16502) from abcam®, (Cambridge, MA). Relative densitometry analyses were performed on the p65 and actin bands with a Quantiscan software program. The ratios of p65 to actin band densities

JPET Fast Forward. Published on June 12, 2012 as DOI: 10.1124/jpet.112.192203
This article has not been copyedited and formatted. The final version may differ from this version.

were determined for each colonic sample. The colonic IL-17 results were expressed as the fold change compared to the value from the PBS treatment group (Fitzpatrick et al., 2008).

Nuclear Binding of STAT3

Nuclear extracts from the colon were prepared, as described previously (Fitzpatrick et al., 2008). We utilized a TransAM™- STAT3 assay kit from Active Motif (Carlsbad, CA). This assay measures the nuclear binding of STAT3 to a consensus binding site (5'-TTCCGGAA-3'). For the assay, we used 20 µg of protein from colonic nuclear extracts. The results are expressed as the absorbance at 450 nm.

Statistical Analyses

The data were analyzed by Graph Pad Prism. Specifically, for the IC_{50} determination (colonic organ culture experiment), we used a non-linear regression analysis. Almost all of the measured parameters (TNBS colitis model) were analyzed by One-way analysis of variance (ANOVA), followed by Bonferroni's multiple comparison test. The exception was the colonic ulcer score data. This data was analyzed by the Kruskal-Wallace test, followed by the Dunn's multiple comparison test. A difference of $p < 0.05$ was considered significant for all these statistical analyses.

Ethical Considerations

Vertebrate Animal Use: The rat TNBS colitis protocol was approved by the IACUC at the Penn State College of Medicine.

JPET Fast Forward. Published on June 12, 2012 as DOI: 10.1124/jpet.112.192203
This article has not been copyedited and formatted. The final version may differ from this version.

Results

Vidofludimus (Vido) Attenuates IL-17 Secretion From Colonic Strips

As shown in figure 1, on day 5 after the intracolonic administration of TNBS to rats, the *ex vivo* secretion of IL-17 was increased 5.6 fold (compare basal IL-17 secretion levels in figures 1A and 1B). Vido (100 μM) significantly inhibited ($p < 0.05$) basal IL-17 secretion from colonic strips of TNBS treated mice (figure 1B). Interestingly, cytokine (IL-1β + IL-23) stimulation resulted in a dramatic up-regulation of IL-17 secretion in colonic strips from either PBS or TNBS treated animals (red bars, figures 1A and 1B). Of note, Vido dose-dependently inhibited cytokine stimulated secretion by colonic strips form PBS or TNBS treated rats. The calculated IC_{50} values were 26.4 μM and < 25 μM for inhibiting IL-17 secretion from colonic strips of PBS and TNBS treated rats, respectively (figure 1).

Oral Administration of Vidofludimus (Vido) Alone Most Effectively Improves Many Parameters of TNBS-Induced Colitis in Rats

The measured parameters of colitis were similar in rats treated with vehicles by the i.p. or orogastric routes. Therefore, the data from these animals were combined for subsequent statistical analyses. In most of the treatment groups, rats gained weight over the six-day study period. However, the mean body weight gain was less in TNBS-treated animals, as compared to rats that received PBS enemas. Of note, Uri/TNBS treated rats showed a slight mean weight loss during the study period. Specifically, weight changes (grams/6 days) were: 21.8 ± 1.4 (Vehicle/PBS, [$p< 0.05$ vs. Vehicle/TNBS]), 5.8 ± 3.5 (Vehicle/TNBS), 9.3 ± 4.4 (Vido/TNBS), -0.5 ± 3.5 (Uri/TNBS) and 7.3 ± 5.0 (Vido + Uri/TNBS).

Representative pictures of the distal rat colon are shown in figure 2. There was no ulceration in the colon of an animal given PBS by enema (panel A). In contrast, the right upper panel of this figure shows a prominent area of ulceration (large boxed area, panel B) in the colon of a

JPET Fast Forward. Published on June 12, 2012 as DOI: 10.1124/jpet.112.192203
This article has not been copyedited and formatted. The final version may differ from this version.

Vehicle/TNBS treated rat. In contrast, smaller areas of ulceration were evident in the colons of animals treated with Vido ± Uri (arrow and smaller boxed area respectively, in panels C and D of figure 2). Figure 3A shows the quantification of the colonic ulcer score data. Specifically, these ulcer scores were: 0.3 ± 0.3 (Vehicle/PBS), 6.0 ± 0.3 (Vehicle/PBS), 3.2 ± 0.6 (Vido/TNBS), 5.4 ± 0.4 (Uri/TNBS) and 4.5 ± 0.8 (Vido + Uri/TNBS). A significant reduction ($p < 0.05$ vs. Vehicle/TNBS) in colonic ulceration was found with Vido treatment. In contrast, colonic ulceration in Vido + Uri treated rats (pink bar) was reduced but not to the degree seen in rats treated with Vido treated (green bar). Uri treatment (blue bar, figure 3A) was ineffective for reducing colonic ulceration.

Colonic thickening is also evident in this tissue specimen from the Vehicle/TNBS treated rat (figure 2). In parallel with the colonic thickening noted in Vehicle/TNBS treated rats, the mean colonic weight was also significantly increased ($p < 0.05$) in these animals compared to the Vehicle/PBS cohort of rats. The mean colonic weight values (grams/5 cm colon) were: 0.24 ± 0.01 (Vehicle/PBS), 1.01 ± 0.25 (Vehicle/TNBS), 0.55 ± 0.09 (Vido/TNBS), 1.14 ± 0.29 (Uri/TNBS) and 0.58 ± 0.18 (Vido + Uri/TNBS). Therefore, treatment with Vido ± Uri also reduced the colonic weight. However, due to some variability in Vehicle/TNBS treated rats, statistical significance was not attained in the Vido treatment groups. Figure 3B shows the total macroscopic colonic score data. This data showed a similar pattern to the colonic ulcer data. Total macroscopic scores (representing a combination of ulceration, adhesions, colonic width, and presence of loose stool/diarrhea) were: 1 ± 1 (Vehicle/TNBS), 125 ± 31 (Vehicle/TNBS), 43 ± 17 (Vido/ TNBS), 124 ± 34 (Uri/TNBS) and 72 ± 26 (Vido + Uri/TNBS). A significant reduction ($p < 0.05$ vs. vehicle/TNBS) in the macroscopic colonic score was found with Vido treatment (green bar). Again, the macroscopic colonic score in Vido + Uri treated rats (pink bar) was reduced, but not to the degree in rats treated with Vido alone (green bar).

JPET Fast Forward. Published on June 12, 2012 as DOI: 10.1124/jpet.112.192203
This article has not been copyedited and formatted. The final version may differ from this version.

As shown in figure 4, intracolonic administration of TNBS to rats resulted in colonic epithelial damage and ulceration (large arrow, panel B). There was evidence of prominent leukocyte influx throughout the mucosa and submucosa, which extended to the muscularis mucosa (small arrow). Histological pathology was less prominent in the colons of rats treated with Vido or Vido + Uri (panels C and D, figure 4). The calculated colonic histology scores (0-12 scale, figure 4E) were: 4.7 ± 0.7 (Vehicle/PBS), 10.0 ± 0.4 (Vehicle/TNBS), 7.6 ± 0.5 (Vido/TNBS), 8.9 ± 0.7 (Uri + TNBS) and 8.1 ± 0.7 (Vido + Uri/TNBS) [$p < 0.05$ vs. Vehicle/TNBS for Vido and Vido + Uri treatment groups].

Colonic MPO was measured as an indicator of neutrophil influx into the colon. Normalized MPO values (fold changes vs. PBS) were: 1.0 ± 0.1 (Vehicle/PBS), 7.5 ± 0.9 (Vehicle/TNBS), 4.5 ± 0.8 (Vido/TNBS), 6.7 ± 0.7 (Uri/TNBS) and 3.0 ± 0.7 (Vido + Uri/TNBS) [$p < 0.05$ vs. Vehicle/TNBS for Vido and Vido + Uri treatment groups].

Oral Vidofludimus (Vido) ± Uridine (Uri) Administration to Rats Resulted in Similar Inhibitory Effects on Colonic STAT3 and IL-17

Treatment of rats with Vido alone, or in combination with Uri, reduced the nuclear binding of STAT3 in the colon. In the case of Vido + Uri treatment, statistical significance ($p < 0.05$) was obtained compared to treatment with Vehicle (figure 5A). The data obtained with the wild-type oligonucleotide (brown bar) control, as well as with the mutated oligonucleotide (gray bar) assay kit control, demonstrates the specificity for measuring STAT3 binding from these colonic samples. In a similar fashion to the STAT3 data, rats treated with Vido ± Uri had lower levels of IL-17 in the colon (Figure 5B). Specifically, normalized values (fold changes vs. PBS) were: 1.00 ± 0.06 (Vehicle/PBS), 1.53 ± 0.12 (Vehicle/TNBS), 1.19 ± 0.11 (Vido/TNBS), 1.31 ± 0.98 (Uri/TNBS) and 1.13 ± 0.14 (Vido + Uri/TNBS) [$p < 0.05$ vs. Vehicle/TNBS for Vido + Uri treatment group].

JPET Fast Forward. Published on June 12, 2012 as DOI: 10.1124/jpet.112.192203
This article has not been copyedited and formatted. The final version may differ from this version.

Interestingly, as shown in figure 6A, individual rats that were treated with Vido alone or Vido plus Uri generally had lower levels of colonic NF-kB p65 expression (i.e., less dense bands on western blots) than did Vehicle /TNBS (designated TNBS) treated animals. The overall quantification of the p65 data is shown in figure 6B. Normalized p65/Actin values were: 1.0 ± 0.1 (Vehicle/PBS), 2.0 ± 0.5 (Vehicle/TNBS), 0.5 ± 0.2 (Vido/TNBS), 2.6 ± 0.9 (Uri/TNBS) and 1.4 ± 0.4 (Vido + Uri/TNBS) [$p < 0.05$ vs. Vehicle/TNBS for Vido/TNBS treatment group]. Therefore, treatment with Vido alone (green bar) had the most profound effect on colonic p65 expression.

Oral Administration of Vidofludimus (Vido) Alone Most Effectively Inhibits the Numbers of CD3+ Colonic_T Cells

Figure 7A shows representative CD3 immunohistochemistry results from the rat colon. In the right upper panel, there are relatively large numbers of CD3+ T cells (brown cellular staining, indicated by arrows) within the ulcerated area of the colon from a Vehicle/TNBS treated rat. In contrast, the numbers of CD3+ T cells were less prominent in the colons of rats treated with Vido alone or concomitantly with Uri (see arrows in panels C and D). This data was quantified, as shown in figure 7E. Specifically, the mean numbers of colonic CD3+ T cells were: 5 ± 1 (Vehicle/PBS), 34 ± 6 (Vehicle/TNBS), 6 ± 2 (Vido/TNBS), 42 ± 10 (Uri/TNBS) and 13 ± 7 (Vido + Uri/TNBS) [$p < 0.05$ vs. Vehicle/TNBS for Vido/TNBS and Vido + Uri treatment groups]. Interestingly, the number of positively stained CD3 T lymphocytes was also significantly ($p < 0.05$) less in the Vido + Uri group of rats as compared to the Uri cohort of animals.

Oral Vidofludimus (Vido) Administration to Rats Modulates the Proliferation but Not Apoptosis of Colonic Leukocytes

Representative leukocyte proliferation results, as determined by PCNA immunohistochemistry, are shown in figure 8. Panel A shows only a few scattered proliferating leukocytes in the colonic lamina propria or submucosa (arrow) from a Vehicle/PBS treated rat. In contrast, large numbers

JPET Fast Forward. Published on June 12, 2012 as DOI: 10.1124/jpet.112.192203
This article has not been copyedited and formatted. The final version may differ from this version.

of proliferating leukocytes, some with the morphological appearance of lymphocytes (left arrow), were evident within the ulcerated area of the colon from a Vehicle/TNBS treated rat (panel B). The presence of proliferating leukocytes was less prominent in the colon of a Vido + Uri treated rat (panel D) and very sparse in an animal treated with Vido alone (panel C). The pattern of PCNA positive cell staining in Uri/TNBS treated rats was similar to that in Vehicle/TNBS treated animals (representative picture not shown in figure 8).

Figure 9 shows representative apoptosis results (TUNEL method) from the rat colon. Panel A shows a few apoptotic leukocytes in the lamina propria (arrows) from a Vehicle/PBS treated rat. However, relatively large numbers of apoptotic leukocytes (denoted by black arrows) were evident within the ulcerated area of the colon from a Vehicle/TNBS treated rat (panel B). In contrast, only fewer scattered apoptotic leukocytes were present in the lamina propria and submucosa of rats treated with Vido alone or in combination with Uri (panels C and D). The pattern of positive apoptotic cell staining in Uri/TNBS treated rats was similar to that in Vehicle/TNBS treated animals (representative picture not shown in figure 9).

JPET Fast Forward. Published on June 12, 2012 as DOI: 10.1124/jpet.112.192203
This article has not been copyedited and formatted. The final version may differ from this version.

Discussion

Previously published data showed that Vidofludimus (Vido) potently inhibited rat DHODH, with an IC_{50} value of 1.3 μM (Kulkarni et al., 2010). Vido also attenuated lymphocyte proliferation, with an IC_{50} value of 12.9 μM, and uniquely blocked PHA-stimulated IL-17 production by PBMC's, with an IC_{50} value of 6 μM (Fitzpatrick et al., 2010a, Kulkarni et al., 2010). Importantly, Vido also improved various parameters of TNBS-induced colitis in mice, including the up-regulation of IL-17 associated with this hapten-induced colitis model (Fitzpatrick et al., 2010a). More recently, we reported activation of STAT3 and NF-κB pathways in the colons of mice with TNBS-induced colitis. Activation of these signal-transduction pathways was normalized in mice that were dosed orally with Vido in the range of 50-200 mg/kg (Fitzpatrick et al., 2011).

In order to better understand the mechanisms responsible for the documented anti-colitis actions of Vido; we tested this drug in our model of TNBS-induced colitis in young rats (Fitzpatrick et al., 2010b). Acute colitis can be induced in these animals by a single intracolonic administration of TNBS (8 mg) in 40% Ethanol. This colitis is characterized by transmural colonic inflammation, submucosal collagen deposition and enhanced production of various cytokines including IL-17 (Fitzpatrick et al., 2010b). Therefore, this animal model of IBD was chosen to further evaluate the anti-colitis profile of Vido *in vivo*.

Specifically, rats were dosed concomitantly with Vido and Uridine (Uri). Other investigators have used this experimental approach to examine the *in vivo* mechanisms of action for leflunomide (another DHODH inhibitor) in rats (Chong et al., 1999). The pharmacological principle of this approach relates to the diminution of endogenous pyrimidine levels in the rat following DHODH inhibition, and the restoration of pyrimidines in the tissue following the i.p administration of uridine at 500 mg/kg (Chong et al., 1999). Since DHODH and pyrimidine biosynthesis play an integral role in lymphocyte proliferation, a significant reversal in the *in vivo* effects of DHODH

JPET Fast Forward. Published on June 12, 2012 as DOI: 10.1124/jpet.112.192203
This article has not been copyedited and formatted. The final version may differ from this version.

inhibition (in the presence of Uri) was in fact observed by other investigators (Chong et al., 1999). However, since IL-17 inhibition by Vido appears to be independent from lymphocyte proliferation *in vitro* (Fitzpatrick et al., 2010a), we speculated that inhibition of lymphocyte proliferation by Vido contributes only partly to its pharmacological effects *in vivo*.

The dose of Vido (60 mg/kg), which was used for this study, was within the effective dose range for attenuating TNBS-induced colitis in mice (Fitzpatrick et al., 2010a). Although, we did not directly measure blood or tissue levels of Vido in this study, the relevant literature suggests C_{max} plasma levels of Vido in the range of 80 to 147 µM, following the oral administration of Vido (30 to 300 mg/kg) in rodents (Kulkarni et al., 2010). Therefore, the oral dose of Vido used in this study likely resulted in peak plasma levels of the drug well in excess of the IC_{50} value (12.9 µM) for inhibiting proliferation in PBMC's (Kulkarni et al., 2010), as well as the IC_{50} value (26.4 µM) for inhibiting cytokine stimulated IL-17 secretion from the rat colon (figure 1).

In agreement with our previous results from a murine model of TNBS-induced colitis, treatment of young rats with Vido over a six-day period resulted in significant reductions in the colonic ulcer score, macroscopic colonic score and colonic histology score (figures 2, 3 and 4). Of note, these parameters of colitis were also reduced in animals treated concomitantly with Vido + Uri, but not to the overall degree as with Vido treatment alone. With regard to the colonic weight data, significant attenuations in this parameter were not attained in either of the Vido treatment groups. Perhaps, this is due to lack of prominent inhibitory effects on edema and/or fibrosis in the colonic submucosa, which contributes to the increased colonic weight in this TNBS colitis model (Fitzpatrick et al., 2010b). In contrast, some other parameters of colitis (colonic MPO and IL-17) were generally comparable in Vido ± Uri treated rats. Specifically, a profound reversal in the pharmacological effects of Vido in the presence of Uri (i.e. to the levels found in Vehicle/TNBS treated rats) could not be observed for any parameters of colitis.

JPET Fast Forward. Published on June 12, 2012 as DOI: 10.1124/jpet.112.192203
This article has not been copyedited and formatted. The final version may differ from this version.

As a whole, these data imply that inhibition of T cell proliferation may only partially explain the anti-colitis effects of Vido. In this regard, other mechanisms also appear to be operative (Fitzpatrick et al., 2010a; Fitzpatrick et al., 2011a).

Recently, intriguing information has been published regarding dual activation of NF-κβ and STAT3 pathways in pathological conditions such as hepatic inflammation and cancer (Danese and Mantovani, 2010; Grivenikov and Karin, 2010; He and Karin, 2011). Interestingly, Sutton and colleagues demonstrated that STAT3 and NF-κB pathways mediated IL-17 production from gamma-delta (γδ) T cells (Sutton et al., 2006; Sutton et al., 2009). Subsequently, they reported that both γδ and CD4+ T cells (via IL-17 production) promoted experimental autoimmune encephalomyelitis (EAE) in mice (Sutton et al., 2009).

Interactions between the NF-κB and STAT3 pathways may also contribute to the pathogenesis of intestinal inflammation/IBD (Danese and Mantovani, 2010). Indeed, activation of these pathways has been described in conjunction with DSS-induced colitis in mice, as well as TNBS-induced colitis in rodents (Bai et al., 2007; Kretzmann et al., 2008; Youn et al., 2009; Fitzpatrick et al., 2011a). Moreover, we have reported that Vido inhibits activation of these intracellular signaling pathways in the mouse colon, as well as in murine splenocytes (Fitzpatrick et al., 2011). Therefore, direct inhibition of these pathways may be another important mechanism by which Vido attenuated the macroscopic and histological parameters of TNBS-induced colitis in rats (figures 2 through 4).

As shown in figures 5 and 6, the nuclear binding of STAT3, the nuclear expression of p65, as well as IL-17 were all increased in the colons of Vehicle/TNBS treated rats. Interestingly, all these parameters were down-regulated within a comparable range, in the colons of rats treated with both Vido alone and in combination with Uri. IL-17 plays a potential integral role in the amplification of intestinal inflammation by stimulating various cell types (e.g., myofibrobalsts and

JPET Fast Forward. Published on June 12, 2012 as DOI: 10.1124/jpet.112.192203
This article has not been copyedited and formatted. The final version may differ from this version.

epithelial cells) to produce pro-inflammatory mediators (IL-6 and IL-8) that amplify intestinal inflammation (Zhang et al., 2006; Strepa and Szczepanik, 2011). Therefore, by attenuating IL-17 levels in the colon (figure 5); Vido also likely affected the amplification of intestinal inflammation that is controlled by IL-17. This statement is supported by the MPO data, which suggested that treatment with Vido alone, or in combination with Uri, significantly attenuated neutrophil influx into the colon.

In order to more directly evaluate its relevant pharmacological actions, Vido (25 to 100 μM,) was also tested for inhibiting IL-17 secretion from rat colonic strips (figure 1). Dual cytokine (IL-1β + IL-23) stimulation of colonic explants resulted in the enhanced secretion of IL-17 (figure 1). Similar results have been reported by other investigators, who utilized CD161+ T cells from patients with IBD (Kleinschek et al., 2009). Our results (figure 1) clearly show that Vido could potently inhibit both basal and dual cytokine stimulated IL-17 secretion from colonic strips of rats with acute TNBS-induced colitis. In this *ex vivo* model, it is less likely that the observed inhibitory effect of Vido is solely dependent upon attenuation of leukocyte proliferation, at the time point (24 hours) at which IL-17 was measured (Reiss and Williams, 1979; Mortsyn et al., 1986). However, we did not directly measure cellular proliferation, in conjunction with this colonic organ culture system.

Our unpublished results suggest that Vido (10 to 100 μM) can inhibit T-lymphocyte proliferation, as well as induce apoptosis *in vitro*, by a p53 dependent mechanism (Hamm et al., 2012). Similar results were reported previously by other investigators, who showed that leflunomide prevented the expansion of activated lymphocytes by interfering with progression through the G1 to S phase of the cell cycle, due to mechanisms involving the accumulation of p53 (Fox et al., 1999). Intriguingly, the relevant literature also suggests that STAT3 and NF-κB play a role in the transcriptional control of proliferation and apoptosis (Bollrath and Greten, 2009). Therefore,

JPET Fast Forward. Published on June 12, 2012 as DOI: 10.1124/jpet.112.192203
This article has not been copyedited and formatted. The final version may differ from this version.

it is possible that effects on proliferation and apoptosis observed in Vido treated T-lymphocytes also involved inhibition of these two signal transduction pathways (Fitzpatrick et al., 2011).

Other investigators have utilized CD3 immunohistochemistry to evaluate treatment effects on T cell numbers in the colon, following the administration of TNBS to rats (Gao et al., 2005). As shown in figure 7, the numbers of CD3+ T-lymphocytes were increased approximately seven-fold in the colons of Vehicle/TNBS treated rats. Of note, rats treated with Vido ± Uri had significantly ($p < 0.05$) less numbers of CD3+ cells in the colon than in rats treated with either vehicle or Uri. However, the inhibitory effect on CD3+ T cells was most pronounced in rats treated with Vido alone. Our results (figure 8) suggest that Vido limited the proliferation of leukocytes in the lamina propria and submucosa of TNBS treated rats. In contrast, Vido did not appear to induce apoptosis of infiltrating leukocytes in the colon (figure 9). However, it may be possible that Vidofludimus could selectively induce apoptosis of only T-lymphocytes, as described in a previous *in vitro* study (Hamm et al., 2012). This possibility could be further investigated in future studies. Based on the data presented in this paper, we propose that the inhibition of CD3+ T-lymphocyte numbers in the Vido treatment groups most likely represents the effects of inhibiting cellular proliferation, as well as directly inhibiting IL-17 production, which would limit amplification of the colonic inflammatory response.

In summary, our data suggests that Vido improves TNBS-induced colonic inflammation by a unique dual mode of action: 1) inhibition of colonic T-cell expansion, and 2) direct suppression of colonic IL-17 production, by inhibition of STAT3 and NF-kB activation. This unique dual mode of action displayed by Vido makes it an attractive candidate as a new therapeutic entity for IBD. Currently, Vido is in clinical trials for IBD. Initial Phase 2 data showed that Vido had a good efficacy and safety profile in IBD patients (Herrlinger et al. 2011). Therefore, Vido may represent a future pharmacological alternative for IBD patients currently being treated with other immunosuppressive drugs.

JPET Fast Forward. Published on June 12, 2012 as DOI: 10.1124/jpet.112.192203
This article has not been copyedited and formatted. The final version may differ from this version.

Acknowledgements

The authors would like to thank Dr. Kang Li (Penn State College of Medicine), who prepared the histological slides (TNBS colitis study).

Authorship Contributions

Participated in research Design: Fitzpatrick, Doblhofer, Ammendola

Conducted Experiments: Fitzpatrick, Small

Performed Data Analyses: Fitzpatrick

Wrote or Contributed to the Writing of the Manuscript: Fitzpatrick, Ammendola

JPET Fast Forward. Published on June 12, 2012 as DOI: 10.1124/jpet.112.192203
This article has not been copyedited and formatted. The final version may differ from this version.

References

Bai A, Hu P, Chen J, Song X, Chen W, Pang W, Zeng Z, and Gao X (2007) Blockade of STAT3 by antisense oligonucleotide in TNBS-induced murine colitis. *Int J Colorectal Dis* **22**:625-635.

Bollrath G and Greten FR (2009) IKK/NF-kB and STAT3 pathways: Central signaling hubs in inflammation-mediated tumour promotion and metastasis. *EMBO Reports* **10**:1314-1319.

Chong AS, Huang W, Liu W, Luo l, Shen J, Xu W, Ma L, Blinder L, Xiao F, Xu X, Clardy C, Foster P, and Williams JA (1999) In vivo activity of leflunomide: Pharmacokinetic analyses and mechanism of immunosuppression. *Transplantation* **68**: 100-109.

Danese S and Mantovani A (2010) Inflammatory bowel disease and intestinal cancer: a paradigm of the ying-yang interplay between inflammation and cancer. *Oncogene* **29**: 3313-332.

Elson CO, Beagley KW, Sharmanov AT, Fujihashi K, Kiyono H, Tennyson GS, Cong Y, Black CA, Ridwan BW, and McGhee JR (1996) Hapten-induced model of murine inflammatory bowel disease: mucosa immune responses and protection by tolerance. *J Immunol* **157**: 2174-2185.

Fitzpatrick LR, Small J, Hoerr RA, Bostwick EF, Maines L, and Koltun WA (2008) In vitro and in vivo effects of the probiotic Escherichia coli strain M-17: Immunomodulation and attenuation of murine colitis. *Br J Nutr* **100**: 530-541.

Fitzpatrick LR, Ludwig D, Hoffmann C, Small J, Groeppel M, Hamm S, Lemstra S, and Ammendola A (2010a) 4SC-101, a novel immunosuppressive drug, inhibits IL-17 and attenuates colitis in two murine models of inflammatory bowel disease. *Inflamm Bowel Dis* **16**: 1763-1777.

Fitzpatrick LR, Meirelles K, Small JS, Puleo FJ, Koltun WA, and Cooney RN (2010b) A new model of chronic hapten-induced colitis in young rats. *J Pediatr Gastroenterol* Nutr **50**:240-250.

Fitzpatrick LR, Small JS, and Ammendola A (2011a) Inhibition of IL-17 release by the novel anti-inflammatory drug vidofludimus involves attenuation of STAT3 and NF-kappa B signaling pathways in murine splenocytes and hapten-induced colitis. *Gastroenterology* **140**: S837.

Fitzpatrick LR, Green C, Maines LW, and Smith CD (2011b) Experimental osteoarthritis in rats is attenuated by ABC294640, a selective inhibitor of sphingosine-kinase-2. Pharmacology **87**: 135-143.

Fox RI, Herrmann ML, Frangou CG, Wahl GM, Morris RE, Strand V, and KIrschbaum RE (1999) Mechanism of action for leflunomide in rheumatoid arthritis. *Clin Immunol* **93**:198-208.

Gao D, Wagner AH, Fankhaenel S, Stojanovic T, Schweyer S, Panzner S, and Hecker M (2005) CD40 antisense oligonucleotide inhibition of trinitrobenzene sulphonic acid induced rat colitis. *Gut* **54**: 70-77.

Grivenikov SI, and Karin M (2010) Dangerous liaisons: STAT3 and NF-κB collaboration and crosstalk in cancer. *Cytokine & Growth Factor Reviews* **21**: 11-19.

He G and Karin M (2011) NF-κB and STAT3-key players in liver inflammation and cancer. *Cell Research* **21**: 159-168.

Hamm S, Henning SW, Hentsch B, Vitt D, Groeppel M, and Ammendola A (2012) Vidoludimus induces p53-mediated apoptosis in activated T cells and inhibits IL-17a and IL-17F expression decoupled from lymphocyte proliferation *J Crohns Colitis* **6** (Supplement 1): S16.

Herrlinger KR, Diculescu MM, Fellerman K, Hartmann H, Howaldt SM, Nikolov R, Petrov A, Reindl W, Otte JM, Stoinov S, Strauch U, Sturm A, Voiosu RM, Ammendola A, Dietrich B, Hentsch B, and Stange E (2011) Efficacy, safety and tolerability of vidofludimus in patients with inflammatory bowel disease: The entrance study. *Gastroenterology* **140**: S588-S589.

Holtmann MH and Neurath MF (2006) From immunologic mechanisms to novel therapeutic approaches in inflammatory bowel disease. *Adv Exp Med Biol* **579**: 227-242.

Holtmann MH, Gerts AL, Weinman A, Galleee PR, and Neurath MF (2008) Treatment of crohn's disease with leflunomide as second-line immunosuppression. *Dig Dis Sci* **53**: 1025-1032.

Kleinscheck MA, Boniface K, Sadevoka S, Grein J, Murphy EE, Turner SP, Raskin L, Desai B, Faubian WA, de Waal Malefyt R, Pierce RH, McClanahan T, and Kastelein RA

(2009) Circulating and gut resident human Th17 cells express CD161 and promote intestinal inflammation. *J Exp Med* **206**: 525-534.

Kretzmann N, Fillmann H, Mauriz JL, Marroni CA, Marroni N, Gallego JG, and Tunon MJ (2008) Effects of glutamine on proinflammatory gene expression and activation of nuclear factor kappa B and signal transducers and activators of transcription in TNBS-induced colitis. *Inflamm Bowel Dis* **14**:1504-1513.

Kulkarni O, Sayyed SG, Kanter K, Ryu MI, Schnurr M, Sardy M, Leban J, Jankowsky R, Ammendola A, Doblhofer R, and Anders HJ (2010) 4SC-101, a novel small molecule dihydroorotate dehydrogenase inhibitor, suppresses systemic lupus erythematosus in mrl-(fas) ipr mice. *Am J Pathol* **176**: 2840-2847.

Lanzarotto F, Carpani M, Chaudhary R, and Ghosh S (2006) Novel treatment options for inflammatory bowel disease: targeting alpha 4 integrin. *Drugs* **66**: 1179-1189.

Mortsyn G, Pyke K, Gardner J, Ashcroft R, de Fazio A, and Bhatal P (1986) Immunohistochemical identification of proliferating cells in organ culture using bromodeoxyuridine and a monoclonal antibody. *J Histochem and Cyt*ochem **34**: 697-701.

Nakase H, Okazaki K, Tabata Y, Uose S, Ohana m, Uchida K, Nishi T, Debreceni A, Itoh T, Kawanami C, Iwano M, Ikada Y, and Chiba T (2001) An oral drug delivery system targeting immune-regulating cells ameliorates mucosal injury in trinitrobenzene sulfonic acid-induced colitis. *J Phrmacol Exp Ther* **298**:1122-1128.

Prajapati DN, Knox JF, Emmons J, Saeian K, Csuka ME, and Binion DG (2003) Leflunomide treatment of crohn's disease patients intolerant to standard immunomodulator therapy. *J Clin Gastroenterol* **37**: 125-128.

Reiss B and Williams GM (1979) Conditions affecting prolonged maintenance of mouse and rat colon in organ culture. *In Vitro* **15**: 877-890.

Reuter BK, Asfaha S, Buret A, Sharkey KA, and Wallace JL (1996) Exacerbation of inflammation-associated colonic injury in rat through inhibition of cyclooxygenase-2. *J Clin Invest* **98**: 2076-2085.

Ruckemann K, Fairbanks LD, Carrey EA, Hawrylowicz CM, Richards DF, Kirschbaum B, and Simmonds HA (1998) Leflunomide inhibits pyrimidine de novo synthesis in mitogen-stimulated t-lymphocytes from healthy humans. *J Biol Chem* **273**: 21682-21691.

Strzepa A and Szczepanik M (2011) IL-17 expressing cells as a potential therapeutic target for treatment of immunological disorders. *Pharmacol Rep* **63**: 30-44.

Sutton C, Brereton C, Keogh B, Mills KH, and Lavelle EC (2006) A crucial role for interleukin (IL)-1 in the induction of IL-17- producing T cells that mediate autoimmune encephalomyelitis. *J Exp Med* **203**: 1685-1691.

Sutton CE, Lalor SJ, Sweeney CM, Brereton CF, Lavelle EC, and Mills KHG (2009) Interleukin-1 and IL-23 induce innate IL-17 production from γδ T cells amplifying TH17 responses and autoimmunity. *Immunity* **31**: 331-341.

Tanabe S, Kinuta Y, and Saito Y (2008) Bifidobacterium infantis suppresses proinflammatory interleukin-17 production in murine splenocytes and dextran sodium sulfate-induced intestinal inflammation. *Int J Mol Med* **22**: 181-185.

Wittig B, Johansson B, Zoller M, Schwarzler C, and Gunther U (2000) Abrogation of experimental colitis correlates with increased apoptosis in mice deficient for CD44 variant exon 7 (CD44v7). *J Exp Med* **191**: 2053-2063.

Youn J, Lee NS, Na HK, Kundu JK, and Surh YJ (2009) Resveratol and picennatol inhibit iNOS expression and NF-kappa B activation in dextran sodium-induced mouse colitis. *Nutr Cancer* **61**: 847-854.

Zhang Z, Zheng M, Bindas J, Schwarzenberger P, and Kollis JK (2006) Critical role of IL-17 receptor signaling in acute TNBS-induced colitis*. Inflamm Bowel Dis* 12:382-388.

Footnotes

This work was supported by funding from 4SC AG, Planegg-Martinsried, Germany.

Some of this work was presented as a poster presentation at the ECCO-IBD conference in Barcelona, Spain (February 16-19, 2012).

Reprint requests should be sent to:

Leo R. Fitzpatrick Ph.D.

Associate Professor of Pharmacology

Penn State College of Medicine

1214 research Boulevard

Hummelstown, PA 17036

E-mail: lfitzpatrick@psu.edu

JPET Fast Forward. Published on June 12, 2012 as DOI: 10.1124/jpet.112.192203
This article has not been copyedited and formatted. The final version may differ from this version.

Figure Legends

Figure 1: Vido inhibits IL-17 secretion *ex vivo*, using a colonic organ culture system. Panel A shows the data from PBS-treated rats, while Panel B is the data from TNBS-treated rats. On day 5 after the intracolonic administration of TNBS to rats, the *ex vivo* secretion of IL-17 was increased 5.6 fold (compare basal IL-17 secretion, black bars in figure 1). Vido (100 μM) significantly inhibited ($p < 0.05$) basal IL-17 secretion from colonic strips of TNBS treated mice (right panel), or PBS treated mice (left panel). Cytokine (IL-1β + IL-23) stimulation (red bars, figure 1) resulted in dramatic up-regulation of IL-17 secretion in colonic strips from either PBS ($n = 3$) or TNBS ($n = 3$) treated animals. Vido (25, 50 and 100 μM) dose-dependently inhibited cytokine stimulated secretion by colonic strips from PBS or TNBS treated rats. The calculated IC_{50} values were 26.4 μM and < 25 μM for inhibiting IL-17 secretion from colonic strips of PBS and TNBS treated rats respectively. The results are the mean ± SE from 11-12 colonic strips, for each treatment condition. The data is expressed as pg/ml (per 24 hours). For statistical analyses: * denotes $p < 0.05$ vs. corresponding cytokines group.

Figure 2: Representative pictures of the distal rat colon on postnatal day 28, five days after animals received either intracolonic PBS or TNBS (8 mg in 40% ethanol) enemas. The colon of a rat from the Vehicle/PBS treatment group (panel A) showed a normal macroscopic appearance. A prominent area of ulceration (large boxed area) was evident in the colon of a Vehicle/TNBS treated rat (panel B). In contrast, smaller areas of ulceration were evident in the colons of animals from the Vido treatment group (arrow in panel C), as well as the Vido+Uri treatment group (small boxed area, panel D).

Figure 3: Colonic ulcer scores (panel A) and macroscopic colonic scores (panel B) are lower in rats treated with Vido ± Uri. Figure 3A shows the colonic ulcer score data. These ulcer scores were: 0.3 ± 0.3 (Vehicle/PBS), 6.0 ± 0.3 (Vehicle/PBS), 3.2 ± 0.6 (Vido/TNBS), 5.4 ± 0.4

JPET Fast Forward. Published on June 12, 2012 as DOI: 10.1124/jpet.112.192203
This article has not been copyedited and formatted. The final version may differ from this version.

(Uri/TNBS) and 4.5 ± 0.8 (Vido + Uri/TNBS). Figure 3B shows the total macroscopic colonic score data. Total macroscopic scores (representing a combination of ulceration, adhesions, colonic width, and presence of loose stool/diarrhea) were: 1 ± 1 (Vehicle/TNBS), 125 ± 31 (Vehicle/TNBS), 43 ± 17 (Vido/ TNBS), 124 ± 34 (Uri/TNBS) and 72 ± 26 (Vido + Uri/TNBS). In the figures, * denotes $p < 0.05$ vs. the Vehicle/TNBS treatment group.

Figure 4: Vido ± Uri treatment improves the altered colonic histolological pathology associated with TNBS administration to rats. The colon of a rat from the Vehicle/PBS treatment group showed a relatively normal histological appearance (panel A). The intracolonic administration of TNBS to young rats resulted in colonic epithelial damage and ulceration (large arrow, panel B). There was also evidence of prominent leukocyte influx throughout the mucosa and submucosa, which extended to the muscularis mucosa (small arrow, panel B). Histological pathology was less prominent in the colons of rats treated with Vido or Vido + Uri (panels C and D). Magnification in the figure is 100-fold. Panel E: The colonic histology scores (0-12 scale) were: 4.7 ± 0.7 (Vehicle/PBS), 10.0 ± 0.4 (Vehicle/TNBS), 7.6 ± 0.5 (Vido/TNBS), 8.9 ± 0.7 (Uri + TNBS) and 8.1 ± 0.7 (Vido + Uri/TNBS). * indicates $p < 0.05$ vs. the Vehicle/TNBS treatment group.

Figure 5: Vido ± Uri administration inhibits colonic STAT3 and IL-17 in TNBS-treated rats. **A)** Treatment of rats with Vido alone, or in combination with Uri, reduced the nuclear binding of STAT3 in the colon. The data obtained with the wild-type oligonucleotide (brown bar) control, as well as with the mutated oligonucleotide (gray bar) assay kit control, demonstrates the specificity for measuring STAT3 binding from these colonic samples. **B)** Rats treated with Vido ± Uri also had lower levels of IL-17 in the colon. Specifically, normalized values (fold changes vs. PBS) were: 1.00 ± 0.06 (Vehicle/PBS), 1.53 ± 0.12 (Vehicle/TNBS), 1.19 ± 0.11 (Vido/TNBS), 1.31 ± 0.98 (Uri/TNBS) and 1.13 ± 0.14 (Vido + Uri/TNBS). In the figures, * indicates $p < 0.05$ vs. the Vehicle/TNBS treatment group.

JPET Fast Forward. Published on June 12, 2012 as DOI: 10.1124/jpet.112.192203
This article has not been copyedited and formatted. The final version may differ from this version.

Figure 6: Vido treatment normalizes colonic NF-kB p65 expression in rats. **A)** Representative western blots are shown in this figure. The p65 densitometry values represent data that were normalized to the corresponding actin bands, in order to account for any differences in the densities of the actin spots. **B)** The overall quantification of the p65 data is shown in this panel. Normalized p65/Actin values were: 1.0 ± 0.1 (Vehicle/PBS), 2.0 ± 0.5 (Vehicle/TNBS), 0.5 ± 0.2 (Vido/TNBS), 2.6 ± 0.9 (Uri/TNBS) and 1.4 ± 0.4 (Vido + Uri/TNBS). * denotes $p < 0.05$ vs. the Vehicle/TNBS treatment group.

Figure 7: Representative CD3 immunohistochemistry photographs from the rat colon. Magnification in the figure is 400-fold. Only a few positively stained cells (brown staining, indicated by arrow) are evident in the colon of a PBS treated rat (panel A). In panel B, there are many positively stained CD3+ T cells (arrows) within the ulcerated area of the colon from a Vehicle/TNBS treated rat. In contrast, the numbers of CD3+ T cells were less prominent in the colons of rats treated with Vido ± Uri (panels C and D). Figure 3E shows the mean numbers of colonic CD3+ T cells were: 5 ± 1 (Vehicle/PBS), 34 ± 6 (Vehicle/TNBS), 6 ± 2 (Vido/TNBS), 42 ± 10 (Uri/TNBS) and 13 ± 7 (Vido + Uri/TNBS). * denotes $p < 0.05$ vs. the Vehicle/TNBS treatment group, while + indicates $p < 0.05$ vs. the Uri/TNBS treatment group.

Figure 8: Representative PCNA immunohistochemistry photographs from the rat colon. Magnification in the figure is 400-fold. Only a few proliferating leukocytes in the colonic lamina propria or submucosa (arrow) were present from a Vehicle/PBS treated rat. Large numbers of proliferating leukocytes, some with the morphological appearance of lymphocytes (left arrow), were evident within the ulcerated area of the colon from a Vehicle/TNBS treated rat (panel B). Evidence of proliferating leukocytes was less in the colon of a Vido + Uri treated rat (panel D) and very sparse in an animal treated with Vido alone (panel C).

JPET Fast Forward. Published on June 12, 2012 as DOI: 10.1124/jpet.112.192203
This article has not been copyedited and formatted. The final version may differ from this version.

Figure 9: Representative TUNEL histochemistry photographs from the rat colon. Magnification in the figure is 400-fold. Figure 9 shows representative apoptosis results (TUNEL method) from the rat colon. Panel A shows a few apoptotic leukocytes in the lamina propria (arrows) from a Vehicle/PBS treated rat. Relatively large numbers of apoptotic leukocytes (denoted by black arrows) were evident within the ulcerated area of the colon from a Vehicle/TNBS treated rat (panel B). In contrast, fewer apoptotic leukocytes were present in the lamina propria and submucosa of rats treated with Vido alone or in combination with Uri (panels C and D).

Figure 1

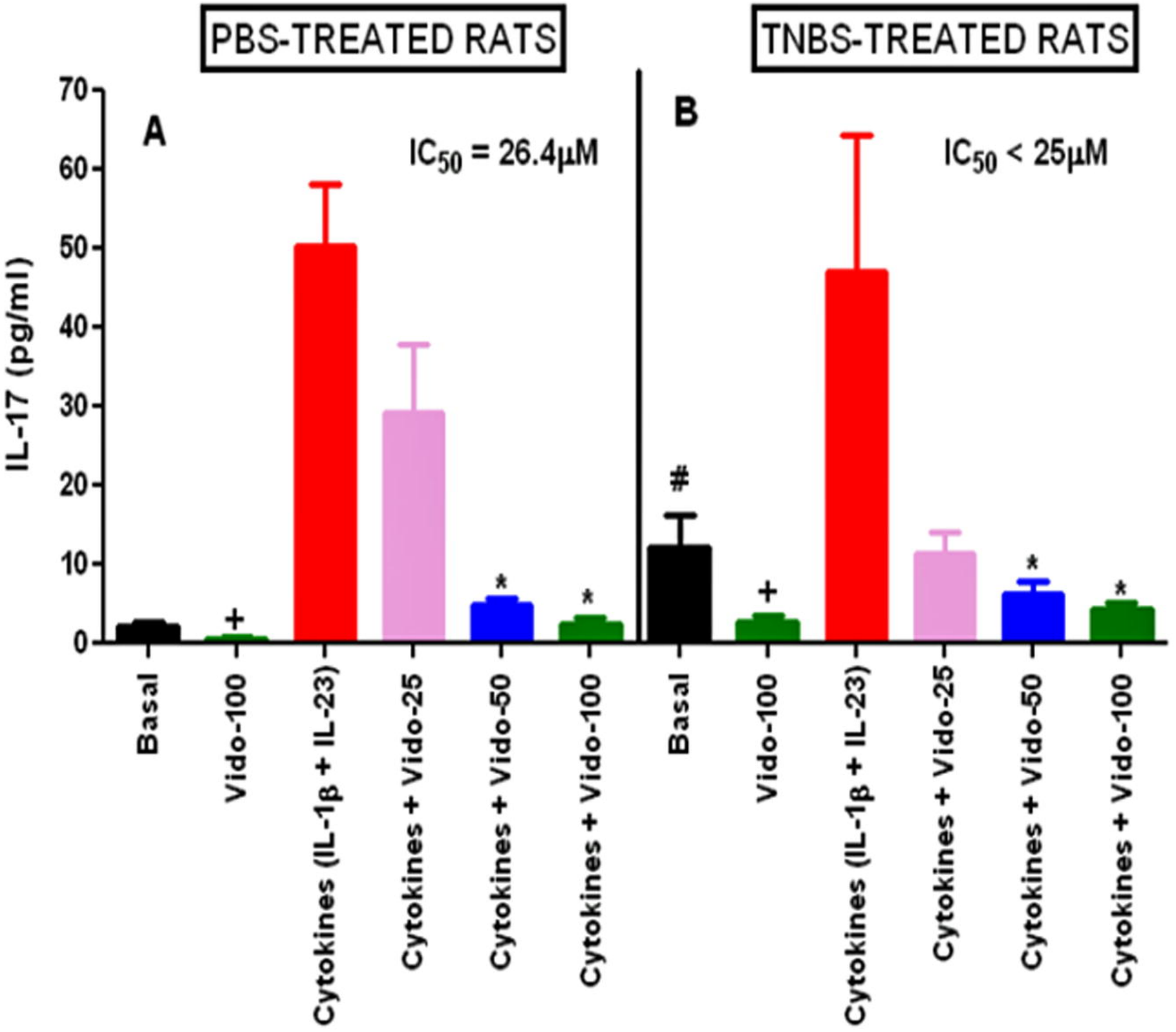
PBS-TREATED RATS
TNBS-TREATED RATS
A
B
IC50 = 26.4µM
IC50 < 25µM
IL-17 (pg/ml)
70
60
50
40
30
20
10
0
#
+
*
Basal
Vido-100
Cytokines (IL-1β + IL-23)
Cytokines + Vido-25
Cytokines + Vido-50
Cytokines + Vido-100

Figure 2

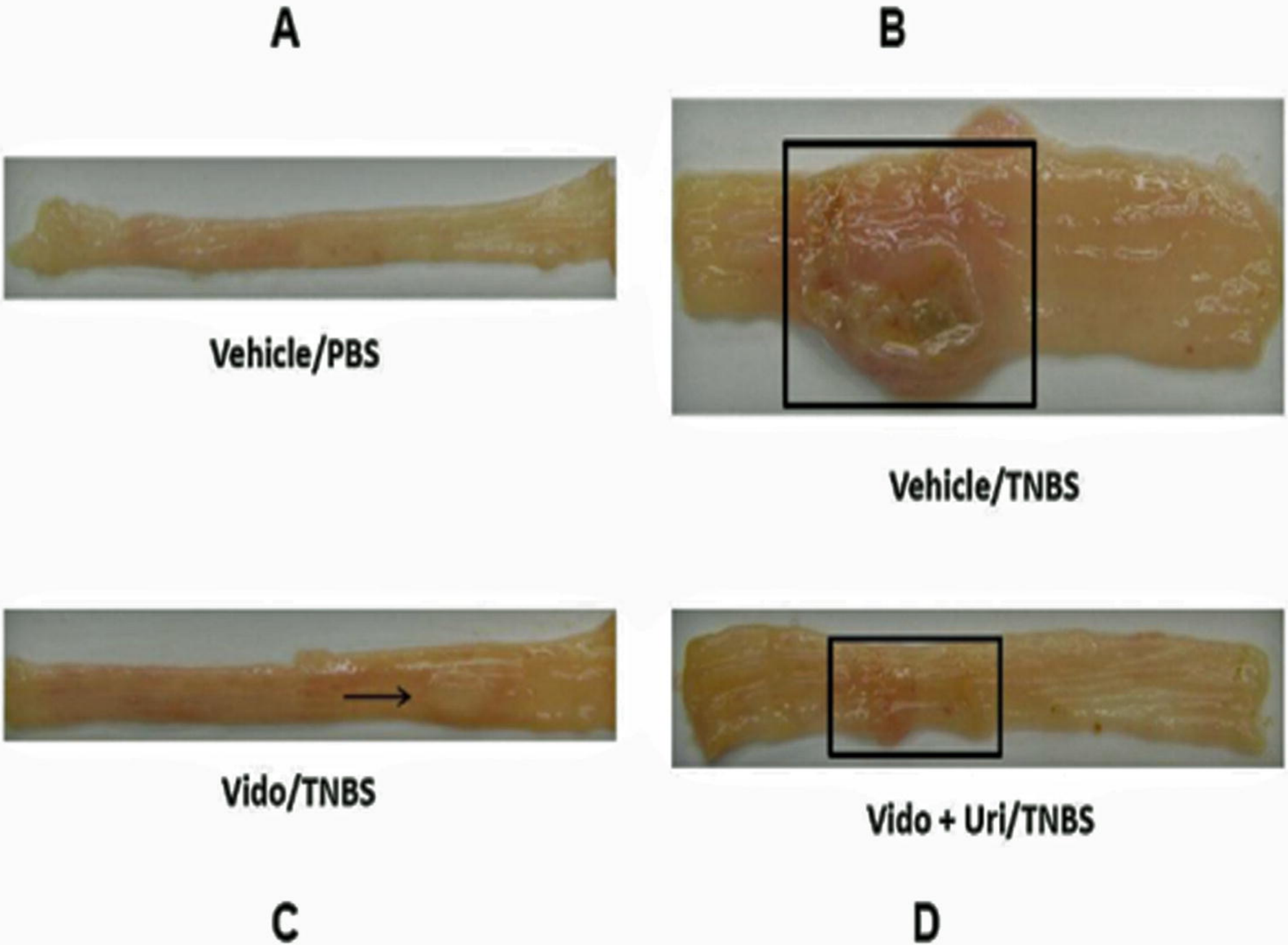

Figure 3

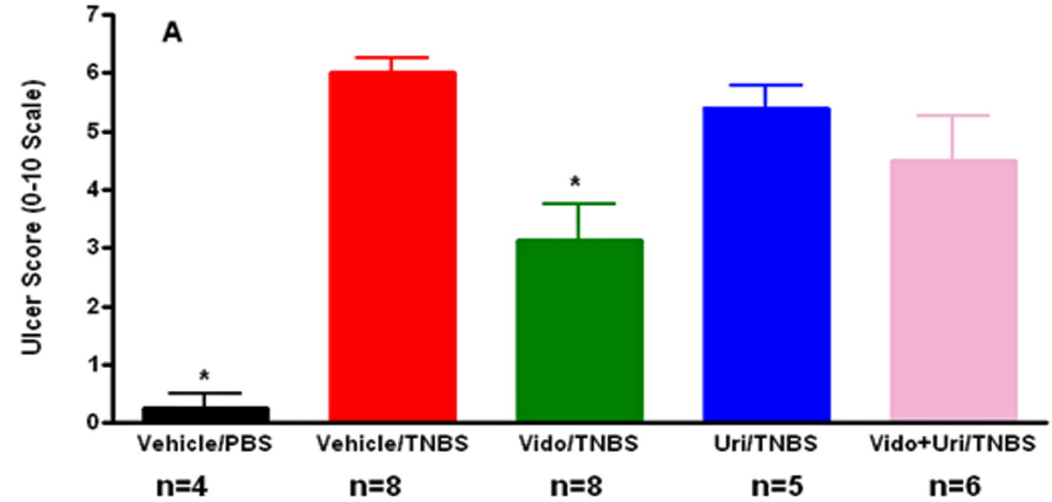
A
Ulcer Score (0-10 Scale)
0
1
2
3
4
5
6
7
*
*
Vehicle/PBS
Vehicle/TNBS
Vido/TNBS
Uri/TNBS
Vido+Uri/TNBS
n=4
n=8
n=8
n=5
n=6

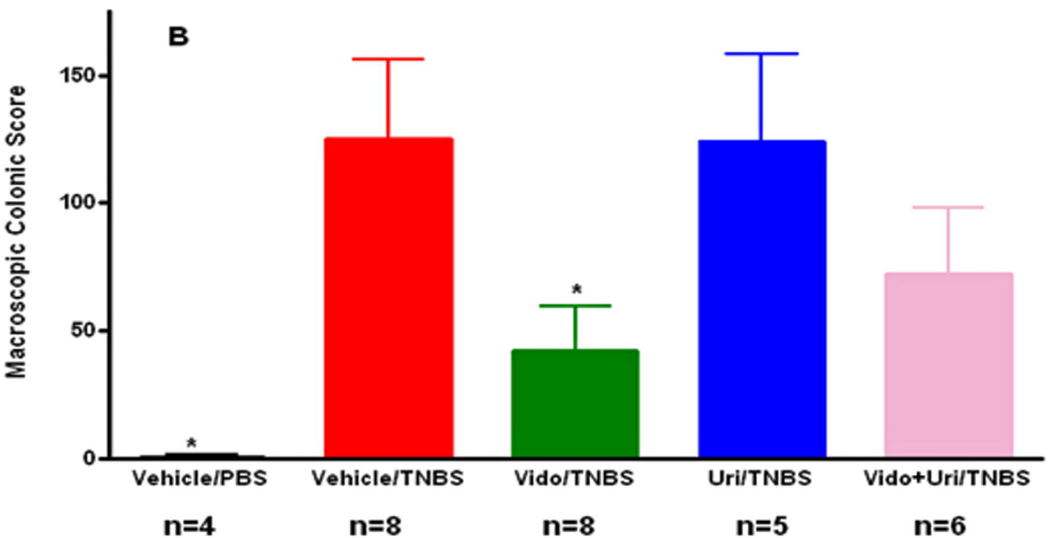
B
Macroscopic Colonic Score
0
50
100
150
*
*
Vehicle/PBS
Vehicle/TNBS
Vido/TNBS
Uri/TNBS
Vido+Uri/TNBS
n=4
n=8
n=8
n=5
n=6

Figure 4

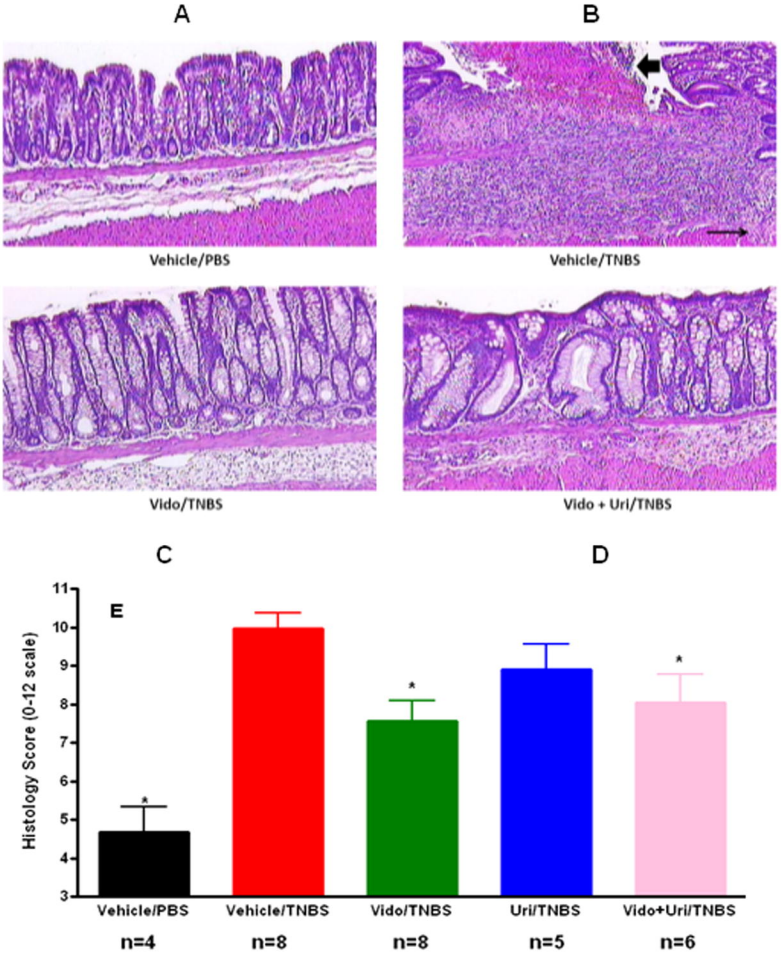
A
B
Vehicle/PBS
Vehicle/TNBS
Vido/TNBS
Vido + Uri/TNBS
C
D
E
Histology Score (0-12 scale)
11
10
9
8
7
6
5
4
3
*
*
*
Vehicle/PBS
Vehicle/TNBS
Vido/TNBS
Uri/TNBS
Vido+Uri/TNBS
n=4
n=8
n=8
n=5
n=6

Figure 5

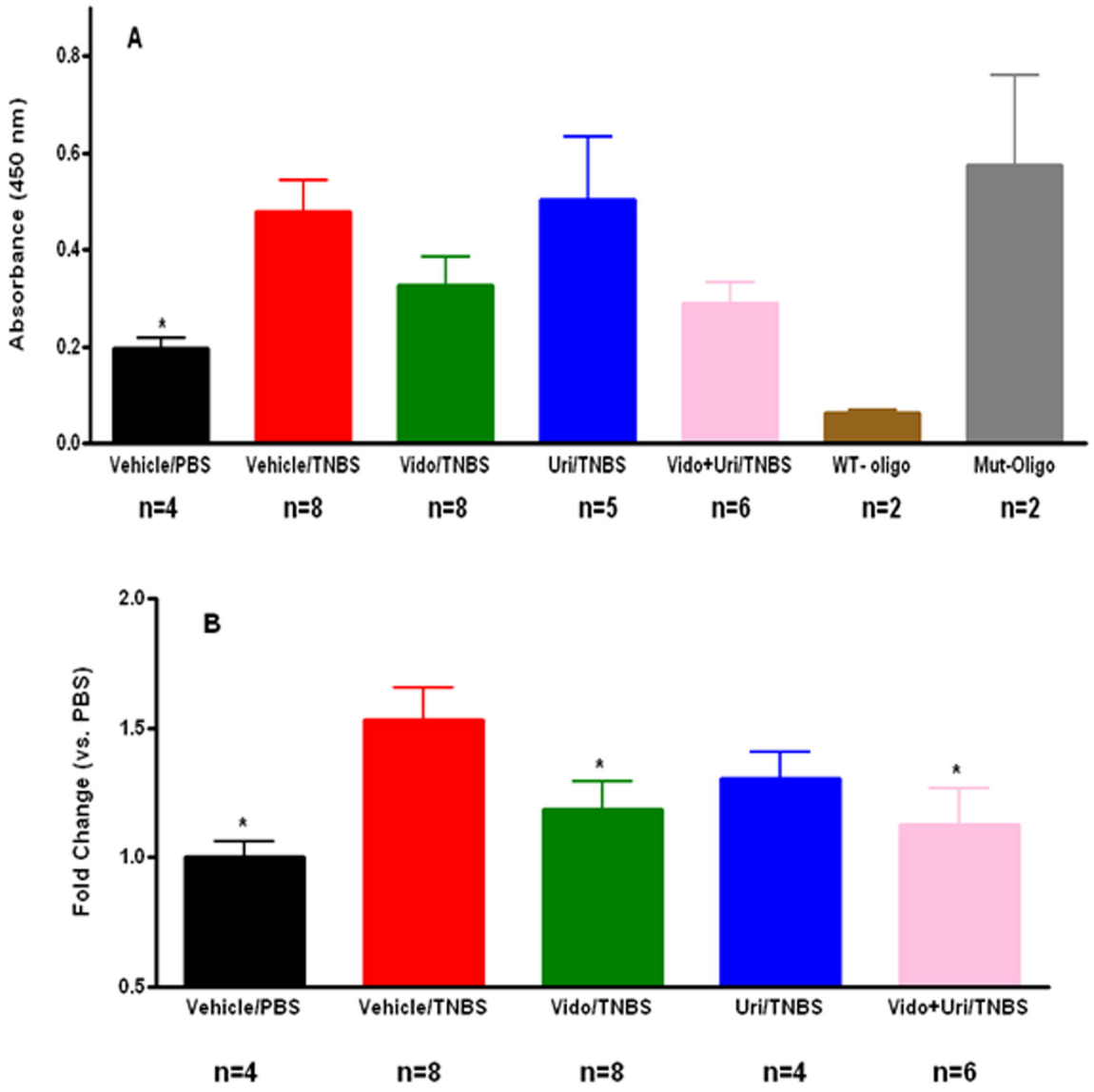

Figure 6

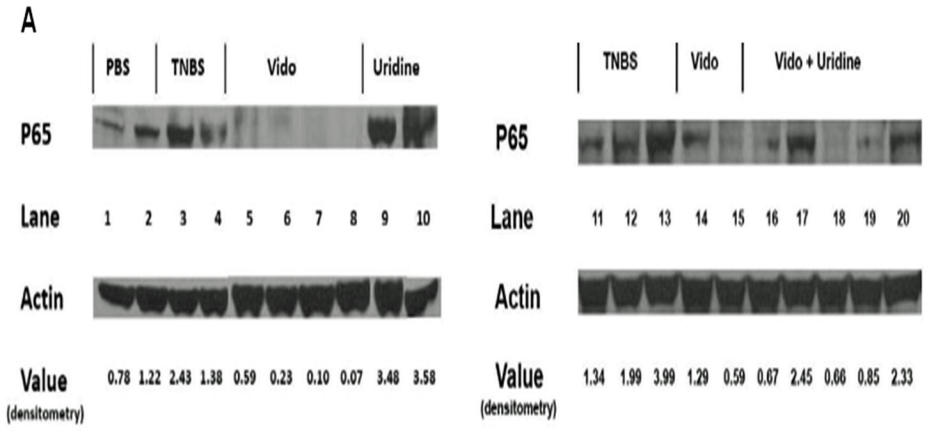
A
PBS
TNBS
Vido
Uridine
P65
Lane 1 2 3 4 5 6 7 8 9 10
Actin
Value (densitometry) 0.78 1.22 2.43 1.38 0.59 0.23 0.10 0.07 3.48 3.58
TNBS
Vido
Vido + Uridine
P65
Lane 11 12 13 14 15 16 17 18 19 20
Actin
Value (densitometry) 1.34 1.99 3.99 1.29 0.59 0.67 2.45 0.66 0.85 2.33

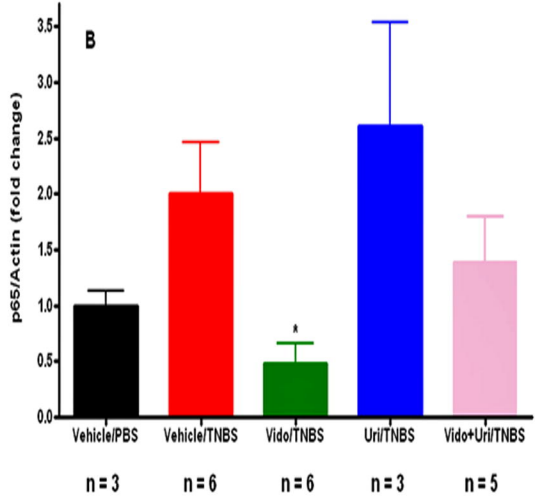
B
p65/Actin (fold change)
3.5
3.0
2.5
2.0
1.5
1.0
0.5
0.0
*
Vehicle/PBS
Vehicle/TNBS
Vido/TNBS
Uri/TNBS
Vido+Uri/TNBS
n = 3
n = 6
n = 6
n = 3
n = 5

Figure 7

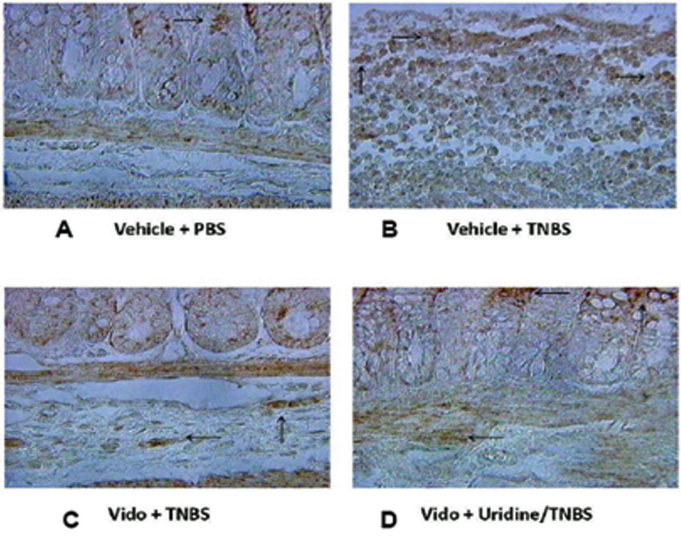
A Vehicle + PBS
B Vehicle + TNBS
C Vido + TNBS
D Vido + Uridine/TNBS
E
Number of CD3+ Cells
50
40
30
20
10
0
*
+
Vehicle/PBS
Vehicle/TNBS
Vido/TNBS
Uri/TNBS
Vido+Uri/TNBS
n = 4
n = 8
n = 8
n = 5
n = 6

Figure 8

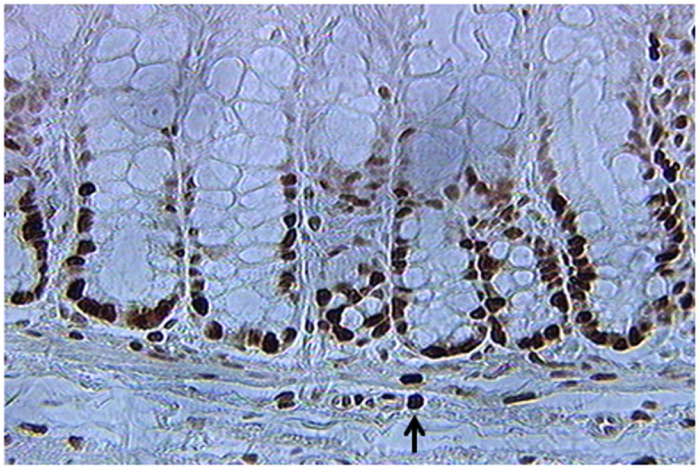

A Vehicle + PBS

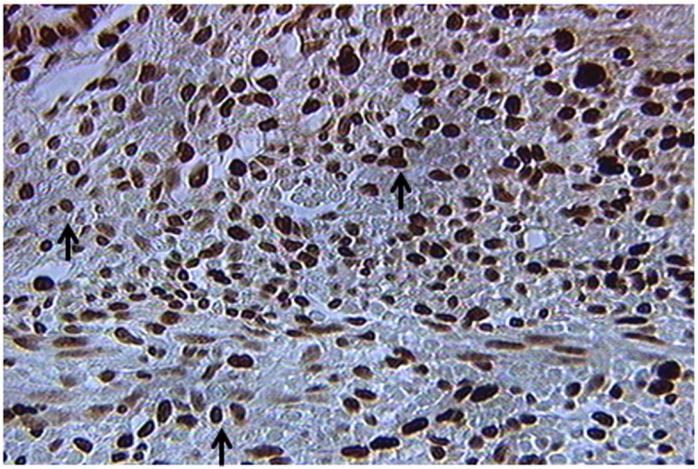

B Vehicle + TNBS

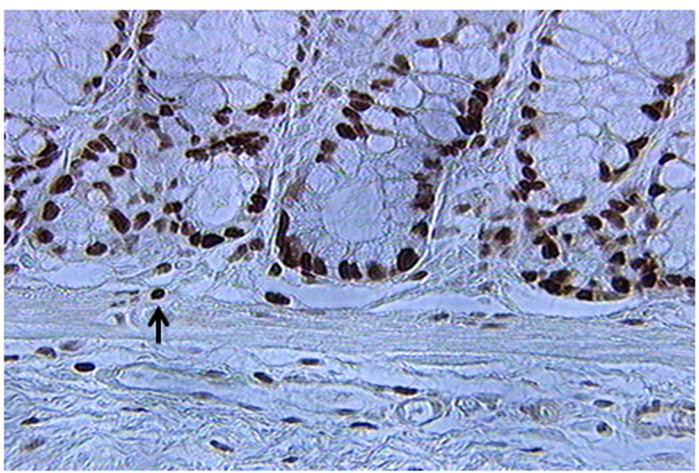

C Vido + TNBS

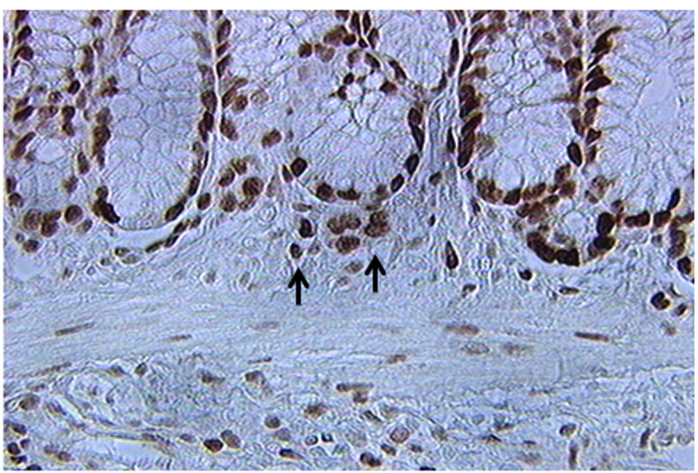

D Vido + Uridine/TNBS

Figure 9

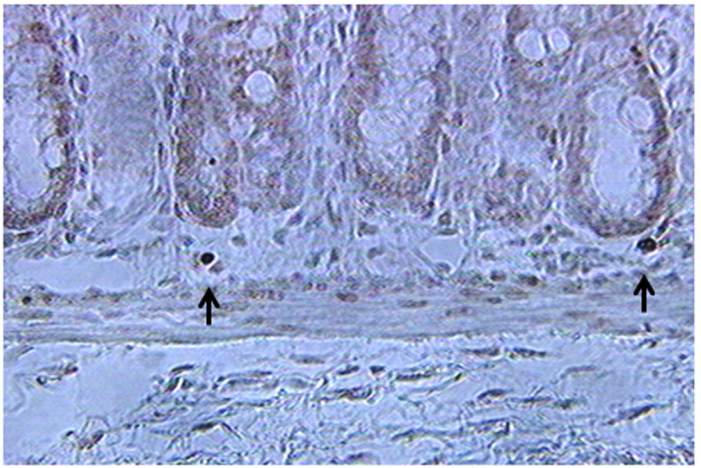

A Vehicle + PBS

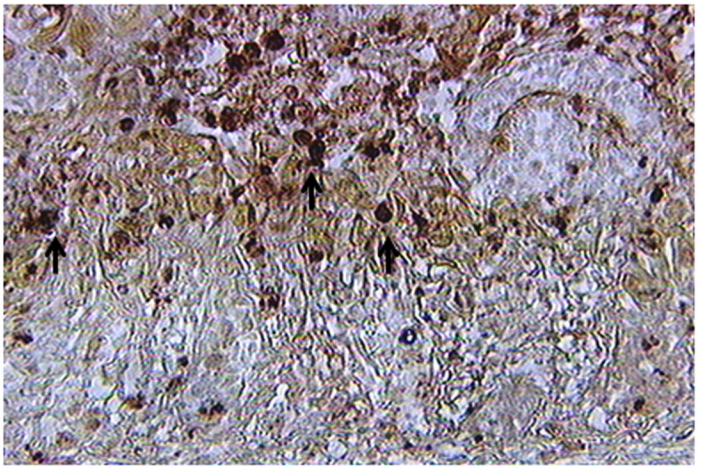

B Vehicle + TNBS

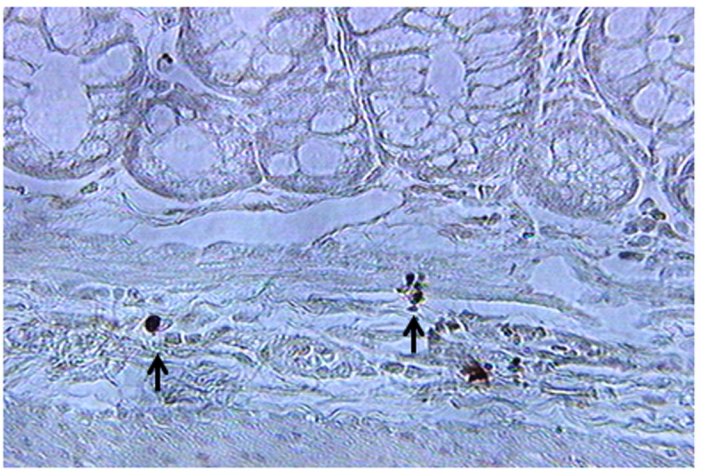

C Vido + TNBS

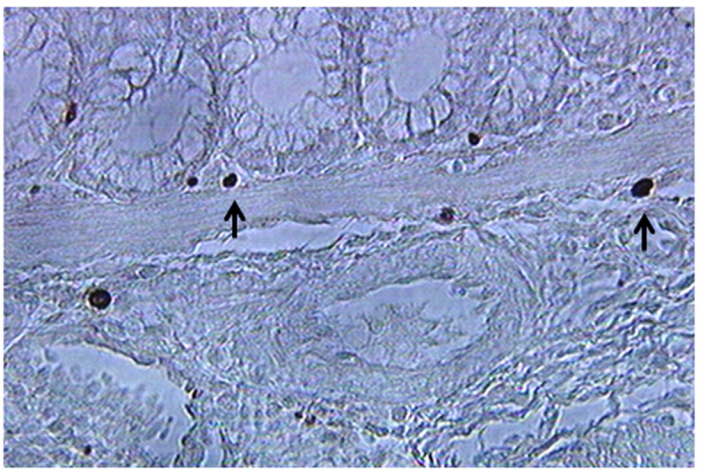

D Vido + Uridine/TNBS